ATMOSPHERIC SCIENCE LETTERS
Atmos. Sci. Let. (2013)
Published online in Wiley Online Library
(wileyonlinelibrary.com) **DOI:** 10.1002/asl2.455

RMetS
Royal Meteorological Society

The prominence of a tropical convective signal in the wintertime Arctic temperature

Changhyun Yoo,[1,*] Steven B. Feldstein[2] and Sukyoung Lee[2,3]

[1] *Center for Atmosphere Ocean Science, Courant Institute of Mathematical Sciences, New York University, New York, NY, USA*
[2] *Department of Meteorology, The Pennsylvania State University, University Park, PA, USA*
[3] *School of Earth and Environmental Sciences, Seoul National University, Seoul, South Korea*

**Correspondence to:*
C. Yoo, Center for Atmosphere Ocean Science, Courant Institute of Mathematical Sciences, New York University, New York, NY, USA.
E-mail: cyoo@cims.nyu.edu

Received: 30 April 2013
Revised: 10 July 2013
Accepted: 10 July 2013

Abstract

Power spectral analysis reveals that the Arctic temperature averaged over 60°N–90°N oscillates on intraseasonal time scales, centered at about 40 days. We present evidence that this intraseasonal peak is strongly tied to the Madden–Julian Oscillation (MJO), the dominant mode of tropical intraseasonal variability. Although an MJO/extratropical surface air temperature relationship has been found in previous studies, our results indicate that this relationship is more prevalent than previously recognized and is strongest at the Arctic surface. This bottom-heavy temperature structure suggests that Arctic surface warming can arise from remote processes, and not necessarily from surface albedo feedback as previously argued.

Keywords: **spectral analysis; Arctic temperature; MJO**

1. Introduction

The Madden–Julian Oscillation (MJO) is a coupled, planetary-scale pattern that includes anomalies of the atmospheric circulation and convection, and propagates eastward with a 30- to 100-day period along the equator (Madden and Julian, 1994; Zhang, 2005). A number of studies have shown that the MJO plays an important role in modulating the extratropical circulation (Weickmann *et al*., 1985; Higgins and Mo, 1997; Cassou, 2008; L'Heureux and Higgins, 2008; Lin *et al*., 2009) via the excitation of poleward propagating Rossby waves (Hoskins and Karoly, 1981; Matthews *et al*., 2004). For East Antarctica, station observations have revealed that there are intraseasonal peaks near 30–50 days in surface wind, surface air temperature (SAT), and surface pressure (Yasunari and Kodama, 1993; Zhou *et al*., 2009). Since there is no known physical process confined to high latitudes which can account for this 30- to 50-day spectral peak, it is plausible that this Antarctic intraseasonal oscillation may stem from tropical variability, such as the MJO. Supporting this possibility, the MJO was found to influence the wintertime Antarctic (Yoo *et al*., 2012b) and Arctic (Yoo *et al*., 2011) SAT. However, in contrast to the Southern Hemisphere, where the MJO influence is confined to the eastern half of Antarctica, in the Northern Hemisphere, the MJO-driven SAT anomaly tends to cover the entire Arctic. This raises the question of how prominent is the impact of the MJO on the entire Arctic region.

This is an important question given the recent debate of whether the decadal Arctic warming trend of the past few decades is more strongly influenced by local or by remote processes (Screen *et al*., 2012 and references therein). While the connection between intraseasonal time-scale teleconnections and decadal climate change may not self-evident, it has been shown previously that decadal changes in the frequency of occurrence of different intraseasonal teleconnection patterns contribute to the decadal Arctic SAT trend (Lee *et al*., 2011). This finding has been reinforced by Yoo *et al*. (2011) who showed that decadal fluctuations in the frequency of the MJO phase (Wheeler and Hendon, 2004) influence the decadal Arctic SAT trend. The case for local process is sometimes made by the fact that the Arctic warming trend is strongest near the surface (Manabe and Wetherald, 1975; Screen and Simmonds, 2010). Because the linkage between the MJO and Arctic SAT takes place through large-scale atmospheric teleconnection patterns (Yoo *et al*., 2012c), if the MJO signature is indeed prominent in the lower tropospheric Arctic temperature field, but less so at higher levels, it would imply that the observed bottom-heaviness in the Arctic temperature trend cannot necessarily be attributed solely to local processes.

2. Data and methods

To calculate power spectra and MJO composite fields, we use the European Center for Medium-Range Weather Forecasts ERA-Interim reanalysis (Dee *et al*., 2011) for 32 recent extended boreal winters (November 1979 through March 2011). We also use the daily real-time multivariate MJO index (RMM), which is defined by the two leading principal components,

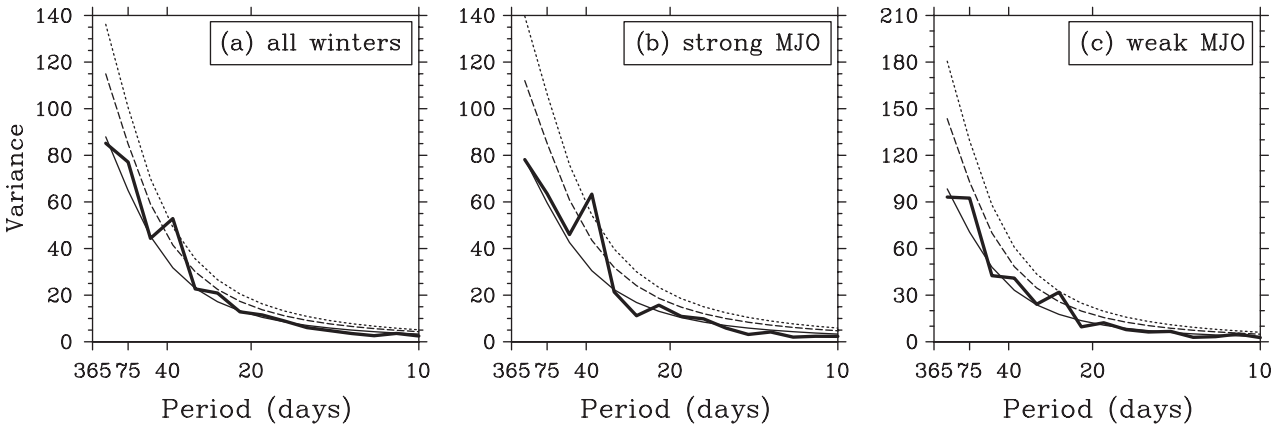

Figure 1. Intraseasonal power spectra (thick solid line) of SAT averaged over 60°N–90°N for (a) all extended boreal winters between 1979 and 2011, (b) strong MJO winters, and (c) weak MJO winters. The strong and weak MJO winters are defined in the text. Also, the red-noise spectrum (thin solid line) and the 95% *a priori* (thin dashed line) and *a posteriori* (thin dotted line) confidence levels are shown.

denoted by RMM1 and RMM2, of the combined empirical orthogonal functions of the intraseasonal 200- and 850-hPa zonal winds and outgoing longwave radiation averaged over the tropical band from 15°S to 15°N (Wheeler and Hendon, 2004). Wheeler and Hendon defined eight phases of the MJO based on the signs of RMM1 and RMM2.

For the power spectral analysis, anomalies are obtained by subtracting the climatological daily mean, which is estimated by the first three harmonics of the calendar mean for each day at each grid point. The power spectra for each winter are averaged to construct a wintertime intraseasonal power spectrum. The red-noise spectrum, and the 95% *a priori* and 95% *a posteriori* confidence levels (Madden and Julian, 1971; Feldstein, 2000) are based on the lag-1 day autocorrelation, which is determined from a least squares fit to the intraseasonal power spectrum. An important feature of power spectral analysis is that for random time series the likelihood of there being at least one spectral peak that exceeds the *a priori* confidence level becomes greater as the number of frequencies retained in the power spectrum increases (if a particular spectral peak in the Arctic SAT was to be expected, then the more commonly used *a priori* confidence level would be most appropriate). As, for the Arctic SAT, there is no *a priori* reason to expect any particular spectral peak in the Arctic SAT, we show both the *a priori* confidence level and the stricter *a posteriori* confidence levels. With regard to the *a posteriori* confidence level, we are evaluating the likelihood of there being at least one Arctic SAT spectral peak that exceeds the 95% *a priori* confidence level.

To construct the composite fields for the MJO, in addition to subtracting the climatological daily mean using the method described above, a 101-point, 20- to 100-day band-pass digital filter is applied. For an MJO event, in addition to the amplitude of the MJO, its eastward propagation is considered (L'Heureux and Higgins, 2008). To be specific, an MJO event is defined to have taken place when all of the following conditions are satisfied: (1) the amplitude of the MJO index is greater than one for consecutive pentads, (2) MJO phases indicate eastward propagation by increasing in numerical order, and (3) MJO events persist for at least six consecutive pentads, but do not remain in one particular phase for more than four pentads. The MJO composite field is neither sensitive to the width of the window of the filter nor to the method of defining an MJO event (Yoo *et al*., 2011).

3. Results

We first examine the power spectra for the SAT averaged over the Arctic region (60°N–90°N). Figure 1(a) shows that the winter power spectrum (thick curve) has a statistically significant ($p < 0.05$, *a posteriori*) peak at approximately 40 days (precisely 37.75 days) [this peak can be seen in tropical outgoing longwave radiation (OLR) power spectra, e.g. Figure 2 in Kiladis and Weickmann, 1992]. At other time scales, the power spectrum closely follows that of a first-order autoregressive process (thin solid curve). Since this spectral peak coincides with the MJO time scale, to explore the possible linkage to the MJO, power spectra of the Arctic SAT are calculated for strong (Figure 1(b)) and weak (Figure 1(c)) MJO winters, where a strong (weak) MJO winter is defined as the seasonal mean MJO amplitude (Wheeler and Hendon, 2004 and references therein) being greater (less) than 1.25. This threshold value divides the 32 winters into 17 strong and 15 weak MJO winters. For the strong MJO winters the 40-day spectral peak strengthens (Figure 1(b)), while for the weak MJO winters this peak diminishes. This result suggests that the 40-day spectral peak in the Arctic SAT is indeed linked to the MJO.

The coherence squared calculated using the RMM1 and RMM2 indices of Wheeler and Hendon (2004) and the Arctic SAT averaged poleward of 60°N provide further support that the 40-day spectral peak in

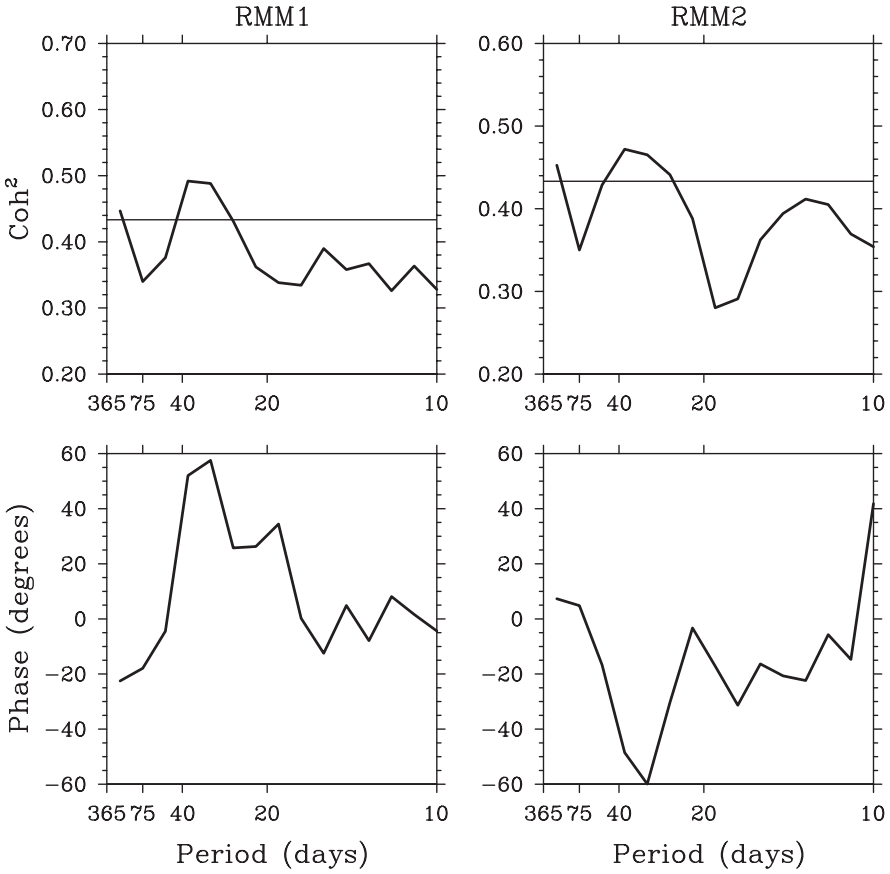

Figure 2. Coherence squared (top row) and phase (bottom row) between the RMM1 and RMM2 indices and Arctic SAT averaged poleward of 60°N. The 90% confidence level for the coherency is shown as a thin line.

Figure 1 is associated with the MJO (top row in Figure 2). The coherence squared for both RMM1 and RMM2 show peaks near 40 days which exceed the 90% confidence level (thin line). The phase relationship indicates that RMM1 leads the Arctic SAT, while RMM2 lags the Arctic SAT (bottom row in Figure 2). This result is consistent with the findings of Yoo *et al*. (2012c) who show that MJO phase 5 (phase 1) is associated with an increased (decreased) poleward wave activity flux.

A linkage between the MJO and Arctic SAT was shown with composite analysis (Yoo *et al*., 2012c). However, that result does not necessarily imply that the Arctic SAT should show a statistically significant spectral peak at the MJO time scale. For example, it was found that the North Atlantic Oscillation (NAO) teleconnection pattern is closely linked to the MJO (Cassou, 2008; Lin *et al*., 2009), yet the power spectrum of the NAO index time series resembles a first-order autoregressive process that lacks any statistically significant spectral peaks at the MJO time scale (Feldstein, 2000). This absence of an MJO time scale spectral peak for the NAO index implies that the driving of the NAO is mostly by other processes, such as synoptic-scale transient eddy vorticity fluxes (Feldstein, 2003). Another extra-tropical process that is strongly influenced by the MJO is the Pacific-North American (PNA) teleconnection pattern (Mori and Watanabe, 2008; Johnson and Feldstein, 2010). Although the PNA index power spectrum shows a spectral peak at the MJO time scale, it just exceeds the $p < 0.05$ *a priori* statistical significance level [Figure 4 of Feldstein (2000)], while the Arctic SAT spectral peak exceeds the $p < 0.05$ *a posteriori* level. As implied by the different significance of these spectral peaks, it is rather remarkable that the relative impact of the MJO is greater on the Arctic than it is on these midlatitude regions, given that the Arctic is more distant from the tropics.

In the same vein, given that the MJO influences the Arctic SAT through atmospheric Rossby wave propagation (Yoo *et al*., 2012a, 2012c), it is also surprising that the MJO spectral peak is stronger for the surface and lower tropospheric temperature fields than it is at higher levels; it can be seen that the 40-day peaks also exist for the lower [700–1000 hPa, Figure 3(i)] and middle [400–700 hPa, Figure 3(f)] tropospheric temperature, but not for the upper tropospheric/lower stratospheric temperature [200–400 hPa, Figure 3(c)]. Meanwhile, the temperature power spectra for midlatitudes [30°N–60°N, Figure 3(b), (e), (h), and (k)] do not show statistically significant peaks. As was discussed earlier, this is presumably due to the relative intensity of non-MJO weather activity, such as midlatitude synoptic-scale storms. In the tropics (0°–30°N, left column), there is a statistically significant spectral

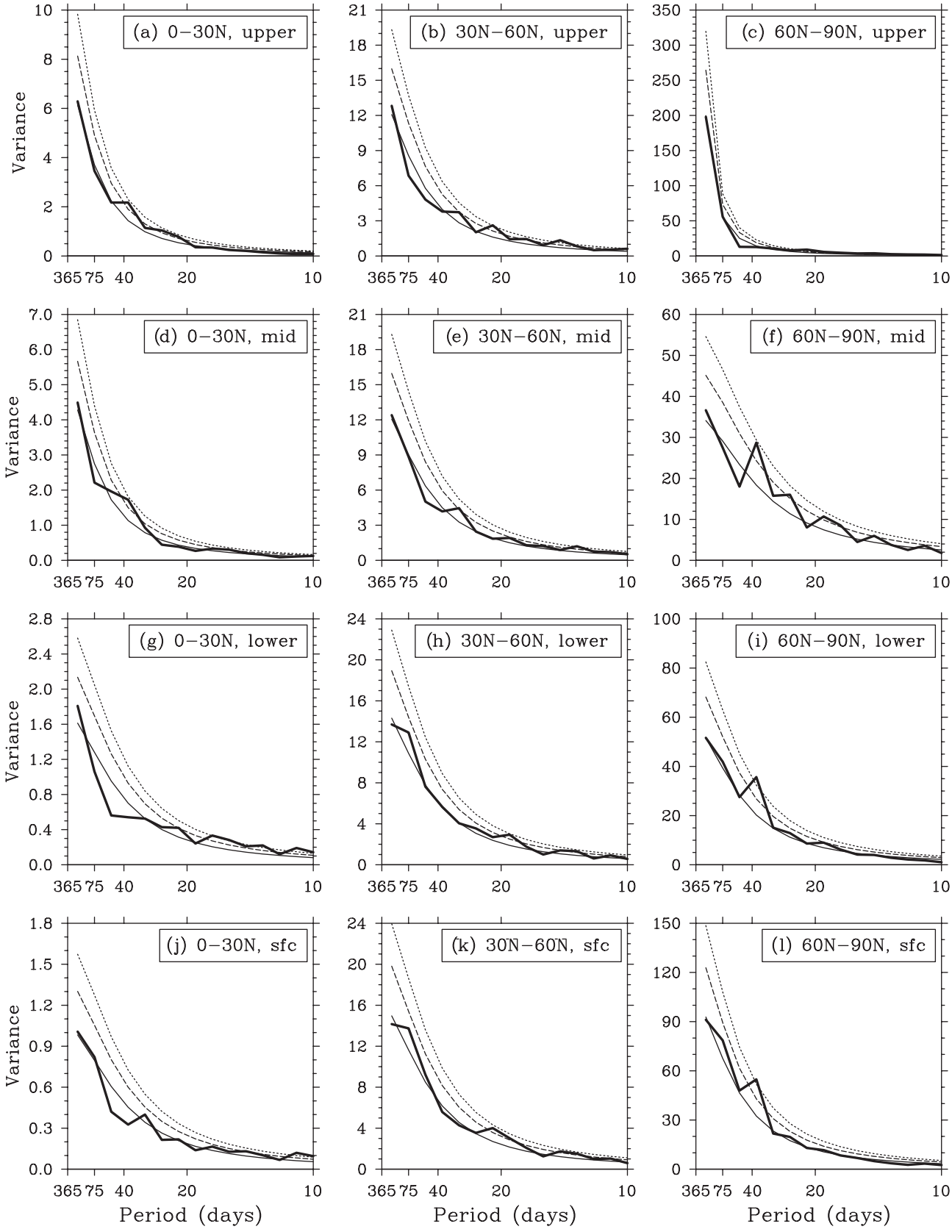

Figure 3. As for Figure 1(a), except for temperature averaged over different levels and ranges of latitudes; upper (200–400 hPa; top row), middle (400–700 hPa; second row), and lower (700–1000 hPa; third row) troposphere, as well as for the surface (bottom row), averaged over 0°–30°N, 30°N–60°N, and 60°N–90°N.

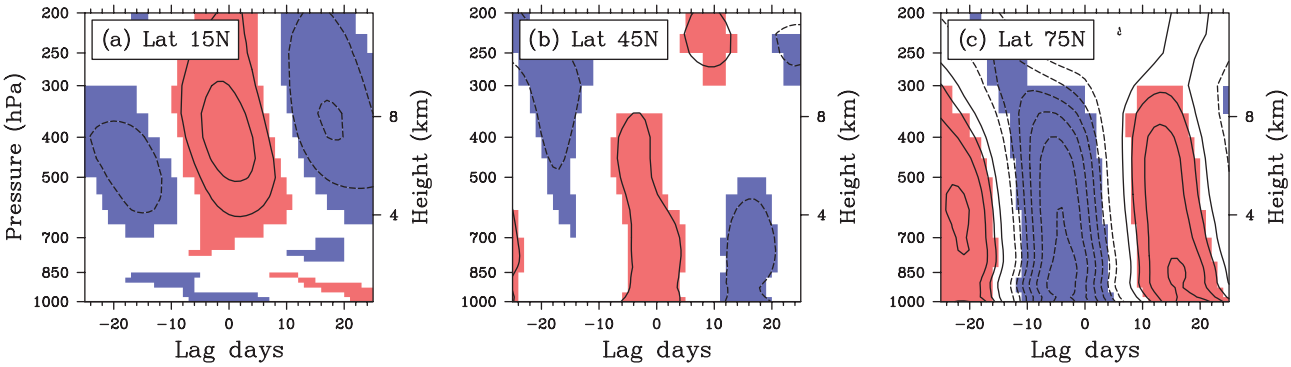

Figure 4. Lagged composites of zonal-mean temperature for MJO phase 5 events at (a) 15°N, (b) 45°N, and (c) 75°N. Solid contours are positive, dashed contours negative, and the zero contours are omitted. Contour interval is 0.1 K. Positive (negative) statistically significant ($p < 0.05$, for a two-sided Student t test) values are shaded in red (blue).

peak at the MJO time scale in the upper and middle troposphere (Figure 3(a) and (d)), but such a peak is absent in the lower troposphere and at the surface (Figure 3(g) and (j)). This top heaviness in the tropics contrasts the bottom heaviness in the Arctic.

A composite analysis provides additional evidence for the top heaviness in the tropics and bottom heaviness in the Arctic. Figure 4 shows lagged composites of the zonal-mean temperature field for MJO phase 5 events (see Section on Data and Methods, where MJO events are defined). Phase 5 is chosen because it was shown to precede Arctic warming (Yoo *et al*., 2011). Consistent with Figure 3, Figure 4 reveals a prominent 40-day oscillation in both the tropical/subtropical upper troposphere and in the Arctic lower troposphere.

4. Discussion and conclusions

The results of this study have implications for the mechanism that drives the recent interdecadal Arctic warming. Screen and Simmonds (2010) argued that since the warming is strongest near the surface, the Arctic warming must be driven by local surface processes, as opposed to remote processes such as poleward heat and moisture fluxes from lower latitudes. Further support for this viewpoint was provided by Screen *et al*. (2012) who performed climate model simulations with prescribed sea surface temperature (SST) and sea ice concentration (SIC) boundary conditions. In one set of model runs, the model was forced with the globally observed SST and SIC. In the second set of model runs, the observed SST and SIC were confined to the Arctic, with climatological values being applied elsewhere. They compared the Arctic temperature trend in the latter model run (as a measure of local forcing) with that computed from the difference between the two model runs (as a measure of remote forcing). A bottom-heavy Arctic warming trend, as in the observations, was found only in the first set of calculations, which suggests that the majority of the Arctic warming trend arises from local forcing. Although it is indeed possible that local processes dominate the Arctic warming trend, since the Arctic SST and SIC may be driven in part by poleward heat and moisture fluxes (Yoo *et al*., 2012a, 2012c), it is also possible that the imposed Arctic SST and SIC in the models used by Screen et al. (2012) may reflect to some extent the impact of the trend in these fluxes. Thus, as previous papers have shown a link between intraseasonal tropical convection and decadal Arctic and Antarctic SAT trends (Lee *et al*., 2011; Yoo *et al*., 2011, 2012b), it is plausible that the interdecadal bottom-heavy temperature trend seen in observations may arise from intraseasonal processes such as the MJO, and not necessarily from a local ice-albedo feedback. Furthermore, the impact of tropical convection on the Arctic temperature also appears to occur at time scales much longer than that of the MJO. For example, as shown in Lee (2012), the more (less) localized tropical SST field of La Nina (El Nino) is associated with Arctic warming (cooling). In summary, our main point is not that local forcing is unimportant, but that remote forcing can also contribute to the bottom-heavy Arctic warming.

Although we focused on the MJO in this work, the fact that the influence of the MJO is substantial enough to show up in the Arctic SAT power spectrum suggests that non-MJO tropical convection may also play a substantial role in regulating Arctic SAT (Lee *et al*., 2011). In fact, principal component analysis of geopotential fields (Supporting Information Figure S1, Appendix S1) shows that there is a pervasive linkage between the Arctic SAT and the upper tropospheric circulation outside of the Arctic. Such findings emphasize the view that skillful model predictions of Arctic climate change depend not only upon an accurate representation of local processes confined to the Arctic but also upon remote process such as tropical convection and the wave trains that link these two regions.

Supporting information

The following supporting information is available:

Figure S1. The leading EOF of intraseasonal surface air temperature poleward of 20°N (a), along with power spectrum of

the corresponding PC (b). Similarly, in (c) and (d), the leading EOF and its corresponding PC are shown for intraseasonal geopotential at 400 hPa. For the left column, positive (negative) values are shaded in red (blue), and the values are shown with solid (dashed) contours. For the right column, the red-noise spectrum (thin solid line) and the 95% *a priori* (dashed line) and 95% *a posteriori* (dotted line) confidence levels are shown.

Appendix S1. Horizontal pattern of leading Arctic surface air temperature EOF and its linkage to teleconnections.

Acknowledgements

The authors appreciate two anonymous reviewers for their constructive comments. The authors also thank the European Center for Medium-Range Weather Forecasts for providing the ERA-interim data and M. Wheeler and H. Hendon for the MJO index. SBF and SL were supported by National Science Foundation grants AGS-1036858 and AGS-1139970.

References

Cassou C. 2008. Intraseasonal interaction between the Madden–Julian Oscillation and the North Atlantic Oscillation. *Nature* **455**: 523–527, DOI: 10.1038/nature07286.

Dee DP, Uppala SM, Simmons AJ, Berrisford P, Poli P, Kobayashi S, Andrae U, Balmaseda MA, Balsamo G, Bauer P, Bechtold P, Beljaars ACM, van de Berg L, Bidlot J, Bormann N, Delsol C, Dragani R, Fuentes M, Geer AJ, Haimberger L, Healy SB, Hersbach H, Hólm EV, Isaksen L, Kållberg P, Köhler M, Matricardi M, McNally AP, Monge-Sanz BM, Morcrette JJ, Park BK, Peubey C, de Rosnay P, Tavolato C, Thépaut JN, Vitart F. 2011. The ERA-Interim reanalysis: configuration and performance of the data assimilation system. *Quarterly Journal of the Royal Meterological Society* **137**: 553–597, DOI: 10.1002/qj.828.

Feldstein SB. 2000. The timescale, power spectra, and climate noise properties of teleconnection patterns. *Journal of Climate* **13**: 4430–4440.

Feldstein SB. 2003. The dynamics of NAO teleconnection pattern growth and decay. *Quarterly Journal of the Royal Meterological Society* **129**: 901–924.

Higgins RW, Mo KC. 1997. Persistent North Pacific circulation anomalies and the tropical intraseasonal oscillation. *Journal of Climate* **10**: 223–244.

Hoskins BJ, Karoly DJ. 1981. The steady-state linear response of a spherical atmosphere to thermal and orographic forcing. *Journal of the Atmospheric Sciences* **38**: 1175–1196.

Johnson NC, Feldstein SB. 2010. The continuum of North Pacific Sea level pressure patterns: intraseasonal, interannual, and interdecadal variability. *Journal of Climate* **23**: 851–867, DOI: 10.1175/2009JCLI3099.1.

Kiladis GN, Weickmann KM. 1992. Circulation anomalies associated with tropical convection during Northern Winter. *Monthly Weather Review* **120**: 1900–1923.

Lee S. 2012. Testing of the Tropically Excited Arctic Warming Mechanism (TEAM) with traditional El Niño and La Niña. *Journal of Climate* **25**: 4015–4022, DOI: 10.1175/jcli-d-12-00055.1.

Lee S, Gong T, Johnson N, Feldstein SB, Pollard D. 2011. On the possible link between tropical convection and the Northern Hemisphere arctic surface air temperature change between 1958 and 2001. *Journal of Climate* **24**: 4350–4367, DOI: 10.1175/2011jcli4003.1.

L'Heureux ML, Higgins RW. 2008. Boreal Winter links between the Madden–Julian oscillation and the Arctic oscillation. *Journal of Climate* **21**: 3040–3050, DOI: 10.1175/2007JCLI1955.1.

Lin H, Brunet G, Derome J. 2009. An observed connection between the North Atlantic oscillation and the Madden–Julian oscillation. *Journal of Climate* **22**: 364–380, DOI: 10.1175/2008JCLI2515.1.

Madden RA, Julian PR. 1971. Detection of a 40–50 day oscillation in the Zonal Wind in the tropical pacific. *Journal of the Atmospheric Sciences* **28**: 702–708.

Madden RA, Julian PR. 1994. Observations of the 40–50 day tropical oscillation, review. *Monthly Weather Review* **122**: 814–837.

Manabe S, Wetherald RT. 1975. Effects of doubling CO2 concentration on climate of a general circulation model. *Journal of the Atmospheric Sciences* **32**: 3–15.

Matthews AJ, Hoskins BJ, Masutani M. 2004. The global response to tropical heating in the Madden–Julian oscillation during the northern winter. *Quarterly Journal of the Royal Meterological Society* **130**: 1991–2011, DOI: 10.1256/qj.02.123.

Mori M, Watanabe M. 2008. The growth and triggering mechanisms of the PNA: a MJO-PNA coherence. *Journal of the Meteorlogical Society of Japan* **86**: 213–236.

Screen JA, Simmonds I. 2010. The central role of diminishing sea ice in recent Arctic temperature amplification. *Nature* **464**: 1334–1337, DOI: 10.1038/nature09051.

Screen JA, Deser C, Simmonds I. 2012. Local and remote controls on observed Arctic warming. *Geophysical Research Letters* **39**: L10709, DOI: 10.1029/2012gl051598.

Weickmann KM, Lussky GR, Kutzbach JE. 1985. Intraseasonal (30–60 day) fluctuations of outgoing longwave radiation and 250 mb streamfunction during Northern winter. *Monthly Weather Review* **113**: 941–961.

Wheeler MC, Hendon HH. 2004. An all-season real-time multivariate MJO index: development of an index for monitoring and prediction. *Monthly Weather Review* **132**: 1917–1932.

Yasunari T, Kodama S. 1993. Intraseasonal variability of Katabatic wind over east Antarctica and Planetary flow regime in the Southern Hemisphere. *Journal of Geophysical Research* **98**: 13063–13070, DOI: 10.1029/92jd02084.

Yoo C, Feldstein S, Lee S. 2011. The impact of the Madden–Julian oscillation trend on the Arctic amplification of surface air temperature during the 1979–2008 boreal winter. *Geophysical Research Letters* **38**: L24804, DOI: 10.1029/2011gl049881.

Yoo C, Lee S, Feldstein S. 2012a. Arctic response to an MJO-like tropical heating in an idealized GCM. *Journal of the Atmospheric Sciences* **69**: 2379–2393, DOI: 10.1175/JAS-D-11-0261.1.

Yoo C, Lee S, Feldstein S. 2012b. The impact of the Madden–Julian oscillation trend on the Antarctic warming during the 1979–2008 austral winter. *Atmospheric Science Letters* **13**: 194–199, DOI: 10.1002/asl.379.

Yoo C, Lee S, Feldstein SB. 2012c. Mechanisms of extratropical surface air temperature change in response to the Madden–Julian oscillation. *Journal of Climate* **25**: 5777–5790, DOI: 10.1175/jcli-d-11-00566.1.

Zhang C. 2005. Madden–Julian oscillation. *Reviews of Geophysics* **43**: RG2003, DOI: 10.1029/2004rg000158.

Zhou M, Zhang Z, Zhong S, Lenschow D, Hsu H-M, Sun B, Gao Z, Li S, Bian X, Yu L. 2009. Observations of near-surface wind and temperature structures and their variations with topography and latitude in East Antarctica. *Journal of Geophysical Research* **114**: D17115, DOI: 10.1029/2008jd011611.

